

Thermodynamic properties of minerals and fluids. Synthesis of minerals

Korepanov¹ Ya.I., Osadchii² V. O., Osadchii¹ E. G. New data on the thermodynamics of silver-gold solid solution in the temperature range 323–673 K

¹Institute of Experimental Mineralogy RAS, Chernogolovka

²M.V.Lomonosov Moscow State University, Department of Geology, Moscow

Abstract. The data were obtained on the activity of silver in the gold and silver alloy by the method of solid AgCl galvanic cell with a solid electrolyte in the temperature range of 323K-673K and atmospheric pressure. In the compositions with a high silver content, positive deviation from ideality was found. Mathematical description of the direct experimental data gave empirical equations for the dependence of the activities of silver and gold in the alloy as functions of temperature and composition. For silver, the following equation was obtained:

$$\ln a_{Ag} = -F \cdot 10^{-3} \cdot (Ax^2 + Bx + C(T)) \cdot (1-x)^2 / (RT)$$

$$\ln a_{Au} = -F \cdot 10^{-3} \cdot (Ax^2 + ((3B - 2A)/3)x + C(T) + B/2) \cdot x^2 / (RT),$$

where $F = 96485.3383$, $R = 8.314472$, $A = 813$, $B = -510$, $C = 223.6 + 0.16786T$, x - the molar proportion of silver in solid solution Ag_xAu_{1-x} .

Key words: solid solution, gold, silver, EMF method, thermodynamic properties.

Citation: Korepanov Ya.I., V.O. Osadchii, E.G. Osadchii (2013). New data on the thermodynamics of silver-gold solid solution in the temperature range 323–673 K 2013

Introduction. The most important work on the thermodynamics of gold - silver solid solution is [White et.al., 1957]. This remarkable work has not lost its importance until present. The main conclusion in [White et.al., 1957] is a negative deviation from the ideal activities of the components in the whole range of temperature and composition. The purpose of this study is to obtain reliable and representative database of the experimental data based on the direct determination of the activity of silver in the alloy in the temperature range of greatest interest for the thermodynamic description of the processes of mineralization. The most important result is the establishment of a positive deviation from the ideal activity of silver in the composition of low gold content in the alloy. The used EMF method is the most accurate one [Osadchii and Rappo, 2004], it does not need a thermodynamic model for analysis of results, just checking interdependent values for consistency.

Theoretical background. Thermodynamic modeling is a powerful tool used for studying the processes of mineralization as well as the subsequent efficient recovery of useful components at the stage of ore concentration. The simulation result is primarily dependent on the availability of experimental data and their quality. EMF method allows the most accurate method to determine the standard thermodynamic functions of the test phase and has been successfully applied to studying the properties of alloys.

Activity of silver a_{Ag} in binary solid solution Ag_xAu_{1-x} can be directly determined by measuring the temperature dependence of the EMF of galvanic cells

(-) Pt|C(graphite)|Ag|AgCl|Ag_xAu_{1-x}|C(graphite)|Pt (+) (A)
using the Nernst equation

$$E = E^0 + \frac{RT}{nF} \ln \frac{a_{Ox}}{a_{Red}} \quad (2)$$

Pure silver on the left corresponds to the oxidized state, and on the right, in the alloy - reduced. This corresponds to the displayed signs of the polarization of the cell (A). The current of silver ions within the cell and the current of electrons in the external circuit are both directed from left to right. Given that standard potential $E_0=0$ (at $a_{Ox}=a_{Red}=1$), $n=1$ - number of electrons in the electrode process and converting finally obtain:

$$\ln(a_{Ag}) = -FE(A)/RT \quad (3)$$

Experiment. Alloy samples weighing approximately 0.6 grams were produced by melting sheet of silver (99.9) and gold (99.9) in quartz ampoules. Alloy in a mold form of a tablet was given a diameter of 6 mm and a height of 2 mm. For homogenization, all samples, in the form of tablets, were annealed in evacuated quartz glass ampoules at 1073 K for a week. Solid electrolyte AgCl (99.999) was also made in the form of tablets, while inert electrodes – from a spectrally pure graphite rod 6 mm in diameter. Elements of electrochemical cells were assembled in a tube-shaped holder made of quartz glass and, to improve the contacts, pressed together with a spring. Silver electrode (reference electrode) was manufactured from a silver rod 3-4 mm in length and 6 mm in diameter. Tablet of solid electrolyte was cut from a block of AgCl, obtained by zone melting method. Elements of the cells were placed in a columnar cell holder (6.5 mm internal diameter) and pressed together with a spring for better contact. Finally, the cell holder was placed in a container made of quartz glass, with pipes for the input and output of the gas. Measurements were carried out in a stream of dry argon (flow rate 0.5-1 m³/min). Plant design and methodology of the experiment are described in detail in [Osadchii and Rappo, 2004]. The holder with the assembled cell was placed in a tubular container made of quartz glass for the circulation of inert shielding gas (argon). Measurements of the EMF $E(T)$ were performed by the thermal titration method, using steps of 50 K in the range of 50 K–400 K. Achieving equilibrium EMF took 10 hours to 10 days at different temperatures and compositions. The equilibrium was considered achieved when EMF values remained constant within $\pm 0.003V$ for a few hours. Temperature dependence of the EMF have been determined in a reversible galvanic circuit (A) with AgCl as a solid electrolyte. Activity of silver in alloy was determined by the equation (2). Measuring the electromotive force of each composition at a fixed temperature was repeated several times in the mode of raising and lowering the temperature. The time to reach equilibrium ranged from 10 hours to 10 days. Thus, the total data array was about 300 $E(T, x)$ points.

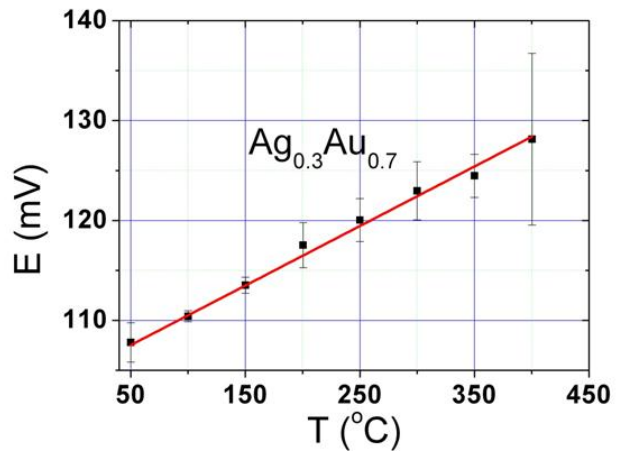
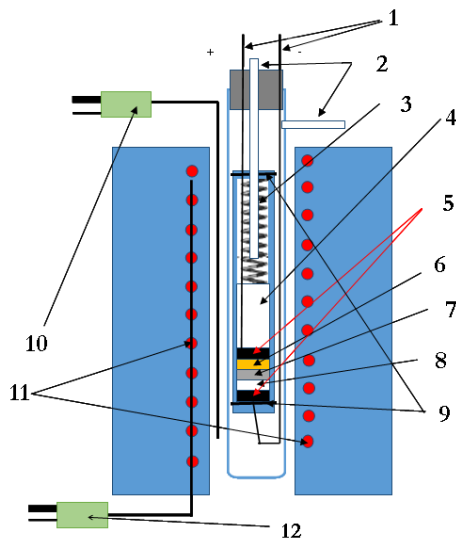


Fig.1. The experimental setup and an example of the experimental data. 1 - platinum wire 2 - tubes for input output of argon, 3 - spring 4 - quartz tube 5 - graphite (inert electrode) 6-sample system (Ag_xAu_{1-x}), 7 - solid electrolyte ($AgCl$), 8 - comparisons (Ag), 9 - ceramic stopper, 10 - Measuring thermocouple, 11 - heating element, 12-thermocouple temperature controller.

Results and discussion. Activity of silver compounds for 11 compositions Ag_xAu_{1-x} ($x = 0.05, 0.1 \dots 0.9, 0.95$) of solid solution have been determined by the method of solid galvanic cells in the temperature range 323-673K and atmospheric pressure of argon.

As a result of processing the whole array of experimental data, it was found that the dependence of the EMF of the cell (A), divided by the square of the mole fraction of gold in the alloy composition, is well described by a parabolic dependence of the form (Fig. 2).

Based on this observation, the results depending on the composition, it was decided to describe an equation (4), and the temperature dependence of the constant term attribute and accordingly, the emf values on the composition and temperature described by the equation:

$$E(A) = (Ax^2+Bx+C(T))(1-x)^2, \quad (4)$$

where $E(A)$ - a voltage in millivolts, x is the mole fraction of the first component in a binary solid solution (in our studies, x corresponds to the content of silver in solid solution Ag_xAu_{1-x}), $C(T)$ is assumed to be a linear function, i.e. $C(T) = a + b \cdot T$.

This approach allows us to describe the change of sign of deviation from the ideal solid solution, which is what we are seeing in the region close to pure silver.

It is not difficult to notice (Fig. 3) a change in the sign of the deviation from the ideal solid solution, which is displayed depending on the activity of the composition as follows (Fig. 4).

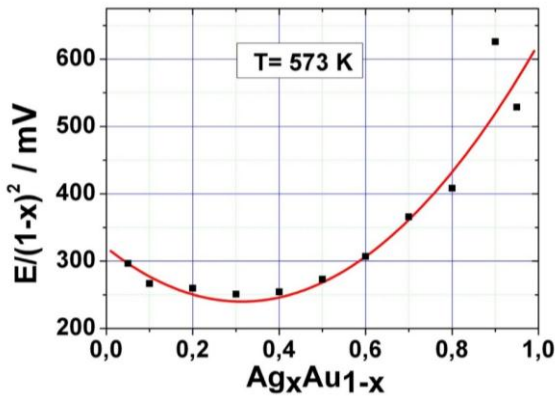


Fig. 2. Dependence $E(A) / (1-x)^2$ of the composition.

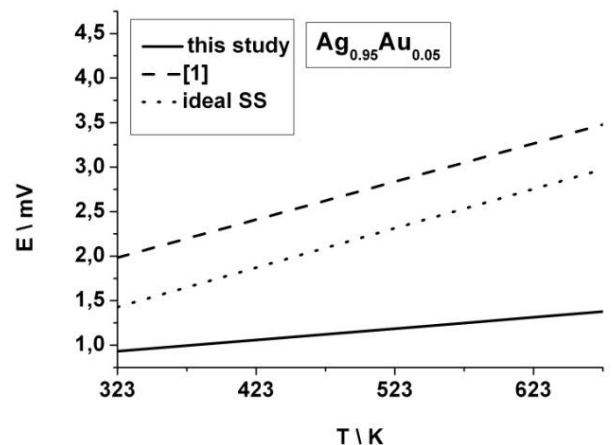
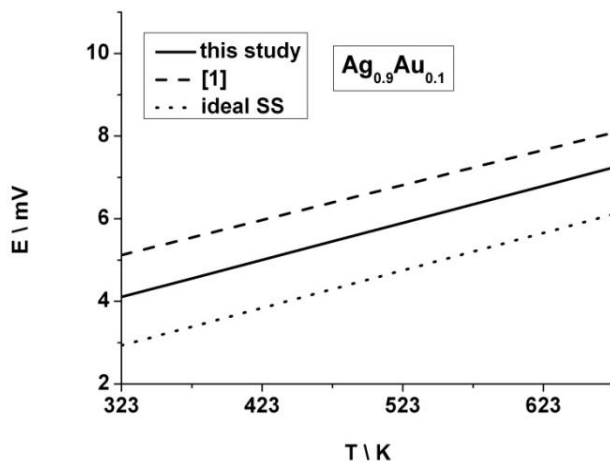


Fig. 3. Illustration of change in the sign of deviation from the ideal solid solution.

To calculate the integral functions, the following formulas were used:

$$G^M = RT \left(x \ln a_x^{Ag_xAu_{1-x}} + (1-x) \ln a_{1-x}^{Ag_xAu_{1-x}} \right)$$

$$G^{EM} = RT \left(x \ln a_x^{Ag_xAu_{1-x}} + (1-x) \ln a_{1-x}^{Ag_xAu_{1-x}} \right) - RT(x \ln x + (1-x) \ln(1-x))$$

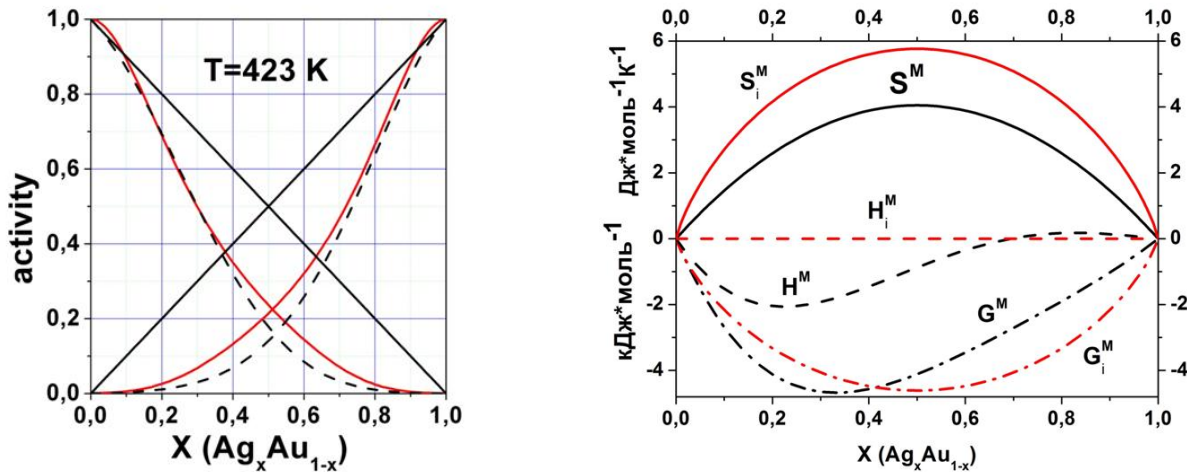


Fig. 4. Compare activities and integral functions with those given in [White, 1957] for the isotherm 423 K.

Conclusion. Thus, the data were obtained on the activity of silver in the gold and silver alloy by the method of solid AgCl galvanic cell with a solid electrolyte in the temperature range of 323K-673K and atmospheric pressure. In the compositions with a high silver content, positive deviation from ideality was found. Mathematical description of the direct experimental data gave empirical equations for the dependence of the activities of silver and gold in the alloy as functions of temperature and composition. For silver, the following equation was obtained:

$$\ln a_{Ag} = -F \cdot 10^{-3} \cdot (Ax^2 + Bx + C(T)) \cdot (1-x)^2 / (RT).$$

Activity of gold in solid solution was calculated from the Gibbs-Duhem equation. When differentiating $\ln a_{Ag}$, we can put aside the factor $(1-x)$, thus avoiding division by 0 (solving the Gibbs-Duhem equation is reduced to taking the integral of a polynomial of degree three). Integrating, we obtain the following formula for the activity of gold:

$$\ln a_{Au} = -F \cdot 10^{-3} \cdot (Ax^2 + ((3B - 2A)/3)x + C(T) + B/2) \cdot x^2 / (RT),$$

where $F = 96485.3383$, $R = 8.314472$, $A = 813$, $B = -510$, $C = 223.6 + 0.16786T$, x - the molar proportion of silver in solid solution Ag_xAu_{1-x} .

This work was partially supported by RFBR (№ № 10-05-00328) and the program number 2 Department of Earth Sciences of RAS.

References :

- Osadchii E. G. and O. A.Rappo (2004). Determination of Standard Thermodynamic Properties of Sulfides in the Ag–Au–S System by Means of a Solid-State Galvanic Cell. *Am. Mineral.*, v. 89, pp. 1405–1410.
- White J. L., R. L.Orr and R.Hultgren (1957). The thermodynamic properties of silver-gold alloys. *Acta Metallurgica*, v. 5, pp. 747–760.

Marina E.A., Mahina I.B., Balitsky V.S. Hydrothermal synthesis of micro-sized Sillenite powders with different chemical composition for creation of optical ceramics on their basis

Institute of Experimental Mineralogy RAS, Chernogolovka

Abstract: A crystals of Sillenites ($Bi_{12}M_xO_{20 \pm \delta}$, where M - the elements of groups II-VIII) has a combination of important physical properties - piezo-, photo- and electro-optical effects, which allows to using it in piezotechnology and optoelectronics. Because the doping of various elements in Sillenite structure have a significant impact on their properties and morphology, the study and production of the various compositions crystals is very important. Sillenites fine-crystalline powder can be used to produce high-quality optical ceramics. This is especially true in the case of incongruent melting sillenites.

Experimental studies were carried out in hydrothermal solutions of different compositions ($NaOH$, NH_4F , H_2O_2). Best results have been obtained in alkaline solutions. Synthesized by spontaneous crystallization of zinc, gallium, iron, silicon, phosphorus and chromium-containing crystals sillenitov size of 0.1-0.7 mm.

Key words: hydrothermal synthesis, Sillenite.

Citation: Marina E.A., I.B.Mahina, V.S.Balitsky (2013). Hydrothermal synthesis of micro-sized Sillenite powders with different chemical composition for creation of optical ceramics on their basis.

A crystals of Sillenites ($Bi_{12}M_xO_{20 \pm \delta}$, where M - the elements of groups II-VIII) has a combination of important physical properties - piezo-, photo- and electro-optical effects, which allows to using it in piezotechnology and optoelectronics. Because the doping of various elements in Sillenite structure have a significant impact on their properties and morphology, the study and production of the various compositions crystals is very important.

The main method of Sillenite crystal growth is crystallization from the melt by the Czochralski method [Kargin 2004]. However, using to this method is difficult to obtain incongruently melting Sillenites, such as Ga-, Al,

Fe - containing Sillenites with better properties than congruently melting sillenites.

The laser ceramics is the most important innovative achievements in the laser materials industry at last years. Such ceramics has better spectral and lasing characteristics than single crystals. Mainly, the optical quality ceramic produces by sintering of the powder of initial oxide components. However, current research indicates that ceramics obtained by sintering of nano- or micro- crystals has better mechanical and optical characteristics [Basiev 2008].

Nanoparticles are often showing the dependence of the properties from the form. At present, various functional materials with desired morphology of nanoparticles synthesized: Pt tetrahedrons, Nb₂O₅ nanotubes, CdS-Ag₂S superlattices, CuO spheres, LiNbO₃ nanosticks etc. Hence the study of synthetic Sillenite crystals morphology is a topical problem.

Zn-, Ga-, Fe-, Si-, P- and Cr-containing Sillenite crystals were synthesized by spontaneous crystallization in hydrothermal solutions with different composition. We

carried out experimental researches at temperature 260° C and pressure 50 MPa in the solution of 10% H₂O₂, 5% NH₄F and 10 % NaOH.

Synthesis was carried out in PTFE ampoules (volume 5 - 8 ml). Six ampoules were placed in a heatproof autoclave also has contact PTFE fettle. The autoclave was filled with the same solution to the same filling factor as the ampoules. Starting material was Bi₂O₃ or NaBiO₃. In addition, in the starting material was placed various additives: C₄H₁₀O₆Zn, Ga₂O₃, Fe₂O₃, SiO₂, Na₃PO₄·12H₂O, K₂CrO₃, Al(OH)₃. The main components (Bi₂O₃ or NaBiO₃) was 95 wt. % of the total mass and one of the above additives was 5 wt. %. Experiments takes from 5 to 10 days. The best Sillenite crystals was synthesized in alkaline solutions.

The research of obtained crystals by electronic-scanning and optical microscopes has showed that Zn-, Ga-, Fe- and Cr-containing crystals grown as a tetrahedron, and silicon and phosphorus Sillenites - as cubes (Fig. 1).

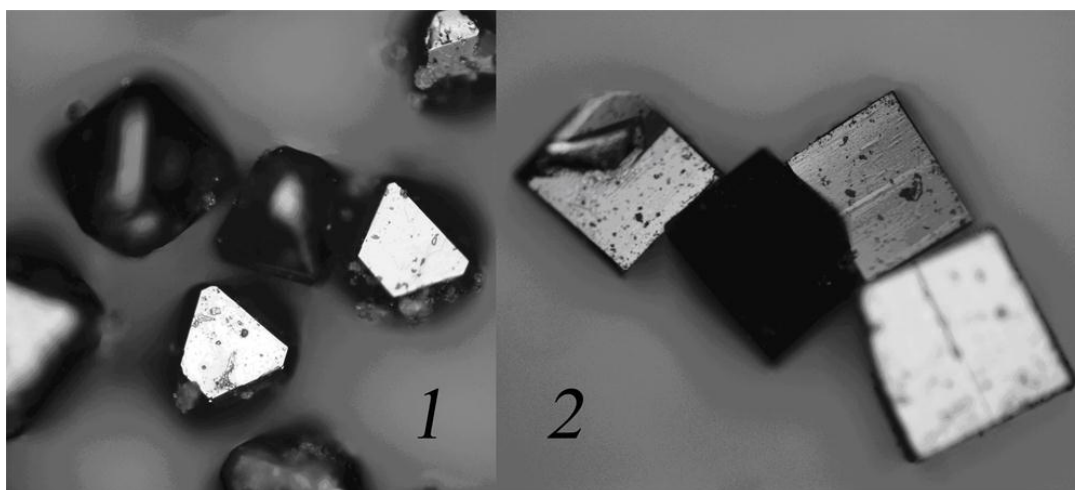


Fig. 1. 1 - Ga-containing Sillenite crystals, 2 - P-containing Sillenite. (By light microscope. Crystal sizes of about 0.3-0.5 mm)

References:

1. Basiev T.T., at al. (2008). Fluoride optical nanoceramics. *Math. RAS, ser.him*, №5, p.863-873.
2. Kargin Y.F. at al. (2004). Crystals with Sillenite structure. Synthesis, structure, properties, Moscow, ABC-2000, p. 316.

Osadchii E.G.^{1, 2}, Bondarenko G.V.¹, Chareev D.A.¹, Osadchii V.O.² Sphalerite solid solution ZnS-FeS: Raman spectra, microhardness and cell parameters

¹ Institute of Experimental Mineralogy RAS, Chernogolovka

² M. V. Lomonosov Moscow State University, Department of Geology, Moscow

Abstract. Sphalerite solid solution crystals (0-6 mol% FeS, 13 samples 1-1.5 mm diameter) were synthesized by the means of vapour transport method. Previously observed rapid increase in the microhardness of sphalerite solid solution from 1.65 to 2.09 GPa has been confirmed. The sphalerites Raman spectra show the regular change of the intensities of the vibrational modes Fe-S and Zn-S in the 250-450 cm⁻¹ wavenumber range. There is also an additional peak 310 cm⁻¹ that is typical for the sphalerites containing less than 6 mol. % FeS. The observed hardening of

sphalerite lattice may be caused by the occupation of vacancies by iron or/and by cluster-formation process.

Key words: sphalerite, Raman spectra, microhardness.

Citation: Osadchii E. G., G. V. Bondarenko, D. A. Chareev, V. O. Osadchii (2013). Sphalerite solid solution ZnS-FeS: Raman spectra, microhardness and cell parameters. *Vestnik ONZ RAS*

A lot of experimental and theoretical studies of sphalerite properties are known [Aswegen & Verleger, 1960; Barton & Toulmin, 1966; Balabin & Sack, 2000; Bryndzia et. Al, 1990; Di Benedetto et. al., 2005, etc.]. The relationship between the cell parameter and the mole fraction of FeS in sphalerite has been studied by many scientists but the obtained data is controversial, except for the fact that cell parameter shows positive deviations from Vegard's law. Although cell parameters measured on the synthetic samples are in agreement with each other the form of the fitting function is still questionable. Available data can be approximated by the second degree polynomial or by two linear functions with interception in the 15-20 mol. % compositional region. [Lepetit et. al, 2003; Osadchii & Gorbaty, 2010].

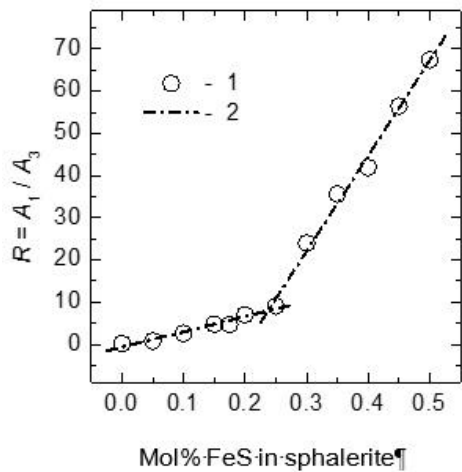


Fig. 1. The ratio of the integrated intensity of the peak at ~295 cm⁻¹ (A₁) to the integrated intensity of the peak at ~345 cm⁻¹ (A₃) as a function of FeS content in sphalerite [Osadchii & Gorbaty, 2010]. 1 – Experiment; 2 – linear fit.

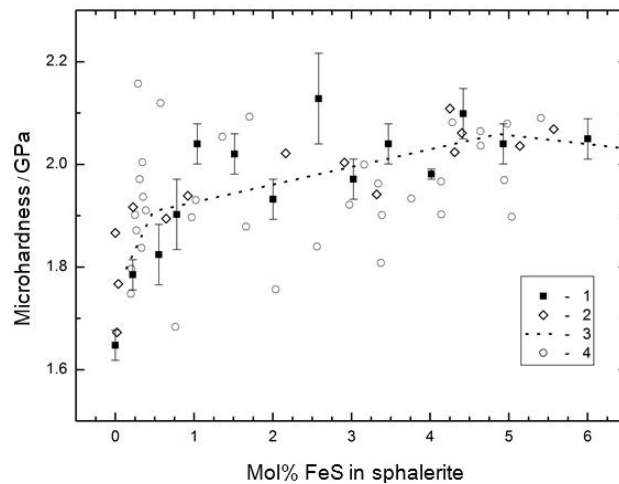


Fig. 2. The microhardness of sphalerite solid solution. 1 – this work; 2 – synthetic samples [Shadlun & Turpenko, 1970]; 3 – by-eye fitting curve [Shadlun & Turpenko, 1970]; 4 – natural samples [Lebedeva, 1972].

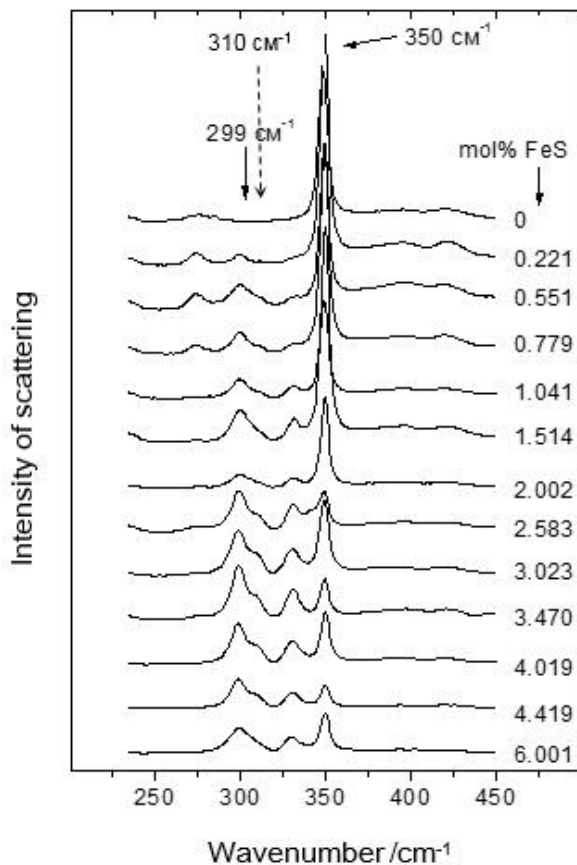


Fig. 3. Raman spectra of sphalerite solid solution.

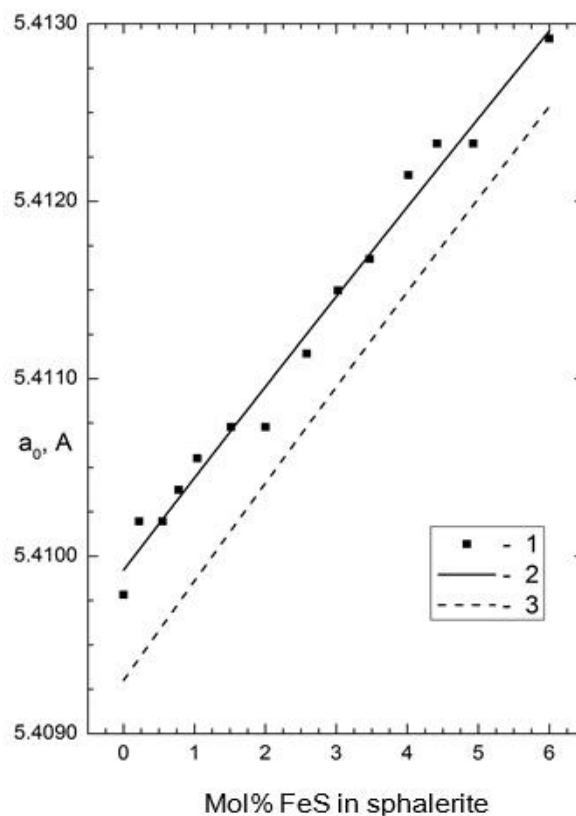


Fig. 4. Spacing curve for iron bearing sphalerites. 1 – This work; 2 – least squares fit: $a_0 = 5.4099 + 5.2278 \times 10^{-4} \times x - 2.7201 \times 10^{-6} \times x^2$, $x = \text{mol.\% FeS in sphalerite}$; no weights used, 3 – curve by [Barton, Toulmin, 1966].

The microhardness of sphalerite is well known [Shadlun, Turpenko, 1970; Osadchii et al., 2012]. There is a rapid growth of microhardness from 1.65 to 2.09 GPa for increasing mol. % of FeS in sphalerite from 0 to 5. It can be caused by occupation of vacancies by iron and thus reducing the quantity of defects in the structure [Osadchii et al., 2012], or it can be connected with some changes in the crystal structure of solid solution [Lebedeva, 1977].

Previous investigations of ZnS-FeS solid solutions by means of Raman [Osadchii & Gorbaty, 2010] spectroscopy were undertaken for 12 sphalerite samples containing 5-50 mol%FeS. The measurements were carried out on powder samples of irregular shape, which significantly hampered the work. It was shown that the ratio of the integral peak intensities is a compositional function (fig. 1). The break shown in the fig. 1 was

interpreted as a sign of a phase transition [Osadchii & Gorbaty, 2010] with the assumption of Fe^{2+} infinite cluster formation in the sphalerite structure.

The inhomogeneity of synthetic and especially natural samples is the main difficulty connected with investigations of sphalerite. It is also difficult to get a series of samples with wide variety of compositions. Thus, the synthesis of relatively large (0.5-1.0 mm) iron-bearing sphalerite crystals containing from 0 to 6 mol. % FeS with compositional step of 0.2-0.5 mol. % FeS was one of the objectives of this study. These samples should be suitable for all kinds of investigations.

Sphalerite solid solution crystals were synthesized at 850°C by means of vapour transport method in evacuated silica glass tubes. The sphalerite solid solutions were prepared by mixing zinc sulfide (99.999%, cubic) with iron sulfide with a small amount of sulfur. Stoichiometric iron sulfide (troilite) was produced by reacting sulfur powder (99.999%) with Fe-carbonyl (99.99%).

Ammonium chloride was used a transport reagent. Silica glass tubes (7-8 cm³) were heated in a horizontal tube furnace. The temperature gradient along the length of the ampoule was about 2-5°C. Full transport of mixture along the glass tube was completed in 20 days. Then, a reversal full transport run was made without opening the tubes. 13 crystals of different iron content and ~1.5 diameter were obtained. Samples were analyzed by means of X-Ray diffraction (XRD) and electron probe microanalysis. No signs of deviation from the given composition were detected.

Microindentation hardness testing (HV) was undertaken to observe the change in sphalerite hardness depending on FeS contents. The measurements are carried out on the PMT-3m device with the load 100 gf. Five crystals of best size and quality were studied in a polished section. Five indentations were made and measured on every crystal. The results are given in fig. 2. Bars show the error (confidence band 99%) of the mean hardness number for each composition.

The scattering of natural sphalerites microhardness is mainly caused by isomorphic and mechanical impurities [Lebedeva, 1972]. Scattering of the data obtained on our synthetic samples and on ones of [Shadlun, Turpenko, 1972] may be due to the anisotropy of hardness and the parting of samples. Anyway, we may clearly see rapid growth of the sphalerite microhardness from 1.65 to 2.09 GPa in the compositional region 0-5 mol. % FeS.

Raman spectra for 13 samples containing from 0 to 6 mol. % FeS were obtained on the Raman microscope «Senterra». The measurements are carried out at room temperature with the following parameters: wavenumber 532 nm, laser output power - 20 mW, spectral slit 50 microns, microscope objective 20^x, accumulation time 30 s. The primary spectra of all samples are given in Fig. 3. Additional peak 310 cm⁻¹ is probably present in all samples containing less than 6 mol% FeS.

Samples were studied by X-ray diffraction on Bruker D8 Advance, Cu-K_{α1}. Unit cell parameters were calculated for the peak (531) with metallic silicon as a standard. The results are given in fig. 4. Our results are ~0.0003 higher than ones given in [Barton&Toulmin, 1966]. In their fitting calculations the pure ZnS cell parameter 5.4093A is given weight of 20. Our calculations show that the pure

ZnS unit cell parameter is 5.4098A which is in good agreement with commonly used nowadays 5.4096A.

The rapid increase in the microhardness of sphalerite containing 0-2 mol. % FeS has been confirmed by measurements on synthetic samples of high quality. Raman spectra have specific features typical for all sphalerites containing less than 2.6 mol% FeS. Observed hardening of sphalerite solid solution lattice with low iron content may due to occupation of structure vacancies by iron. Additional investigations of Raman spectra from temperature of liquid nitrogen up to 400°C are needed to find correlation between observed phenomena.

This research is funded by Russian Foundation for Basic Research 13-05-00405 and by the program №9 of Department of earth Sciences RAS.

References:

1. Aswegen J. T. S. and H. Verleger (1960). Rentgenographische Untersuchung des Systems ZnS-FeS. *Naturwiss.*, 47(6), 131.
2. Balabin A. I. and R. O. Sack (2000). Thermodynamics of (Zn, Fe)S sphalerite. A CVM approach with large basis clusters. *Mineral.Mag.*, 64, 923-943.
3. Barton P. B. and P. Toulmin (1966). Phase relation involving sphalerite in the Fe-Zn-S system. *Econ. Geol.*, 61, 815-849.
4. Bryndzia L. T., S. D. Scott and P. G. Spry (1990). Sphalerite and hexagonal pyrrhotite geobarometer correction in calibration and application. *Econ. Geol.*, 85, 408-411.
5. Di Benedetto F., Andreozzi G. B., Bernardini G. P., Borgheresi M., Caneschi A., Cipriani C., Gateschi D. and Romanelli M. (2005). Short-range order of Fe²⁺ in sphalerite by ⁵⁷Fe Mossbauer spectroscopy and magnetic susceptibility. *Phys. Chem. Minerals*, 32, 339-348.
6. Lepetit P., K. Bente, T. Doering and S. Luckhaus (2003). Crystal chemistry of Fe-containing sphalerites. *Phys. Chem. Minerals*, 30, 185-191.
7. Osadchii E.G. and Y.E. Gorbaty (2010). Raman spectra and unit cell parameters of sphalerite solid solutions (Fe_xZn_{1-x}S). *Geochim. Cosmochim. Acta*, 74, 568-573.
8. Lebedeva S. I. (1972). The typomorphic properties of sphalerites from the deposits of various ore formations. *Tipomorphism mineralov i ego prakticheskoe znachenie*, Moscow, 80-83 (In Russian)
9. Lebedeva S.I. (1977). Microhardness of minerals, Moscow, Nedra, 118 p. (In Russian)
10. Osadchii V.O, D. A. Chareev, E. G. Osadchii (2012). Microhardness of sphalerite solid solution (Zn,Fe)S. *Abstracts of all-Russian annual seminar of experimental Mineralogy, Petrology and Geochemistry*, Moscow, GEOKHI, 17-18 april 2012, 70-71.
11. Shadlun T. N. and S. A. Turpenko (1970). A note on a connection between microhardness of sphalerite and its iron content. *Doklady. AN SSSR*, 194, № 6, 1412-1414.

Redkin A.F. Chemical composition influence on crystal lattice constant of pyrochlores

Institute of Experimental Mineralogy RAS, Chernogolovka

Abstract. The influence of mol fraction and nature of the cations in the site B of pyrochlores on the lattice constants (LC) for Na⁺, Ca²⁺, U⁴⁺, Nb⁵⁺, Ta⁵⁺, Ti⁴⁺, Sb⁵⁺, Zr⁴⁺, V³⁺, V⁴⁺, W⁵⁺, W⁶⁺

Abstracts

substituted pyrochlores obtained by hydrothermal synthesis in 1*m*NaF at 800°C, *P*=200 MPa, and under controlled oxidizing conditions was considered. It was found that dependence of LC from mol fraction of the cation is linear for the pyrochlores where less than 0.5 moles of Nb⁵⁺ (or Ta⁵⁺) were replaced.

Key words: hydrothermal synthesis, pyrochlores, lattice constant.

Citation: Redkin A.F. (2013). Chemical composition influence on crystal lattice constant of pyrochlores. Electron. Scien. - Inform. J. "Vestn. Otd. nauk Zemle RAN", No

Pyrochlores are both minerals and synthetic chemical compounds described by formula A_{2-*m*}B₂O₆(O, OH, F)_{1-*n*}·*p*H₂O (where A – cations with the charge (*Z*) from +1 to +4 and crystalline radius 1.1–1.5 Å; B – cations with *Z* from 3 to 5 and R_B = 0.7–0.9Å; Y – anions O²⁻, OH⁻, F⁻; *m* = 0.0–1.7, *n* = 0.0–1.0 and *p* = 0.0–2.5), belong to cubic system and space group *Fd* $\bar{3}$ *m* [Hogarth, 1977, Atencio et al., 2010]. The typical form of pyrochlore is octahedron. The main pyrochlore characteristic is a lattice constant (LC \equiv a₀). The natural pyrochlores are multicomponent

substances and the contribution inclusion of each cation in LC is a difficult task. Previously [Chakoumakos, 1984], the data on the synthetic pyrochlores (obtained mostly by the dry synthesis) were analyzed. The influence of dimensions parameters (interatomic spacing between cation and anion A-O, B-O) on LC was examined and the limiting values of a₀ were set up.

In the pyrochlore structure each B cation is surrounded by six O²⁻ anions forming octahedron (Fig. 1). But O²⁻ anions, forming a chain with B cations change their position relative to the B-B-B line. As a result, the chain of octahedrons represents a broken line in the XZ plane at constant Y. In spite of the structure of pyrochlore is shown by the spheres representing the ions of corresponding radii, the B-O bond is probably more covalent than ionic. The interatomic spacing R_{B-O} ≤ R_B + R_O and any cations substitution in B position must have an influence on LC.

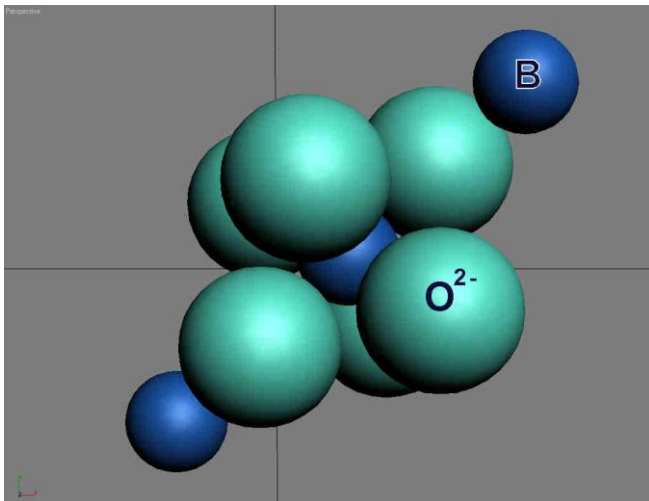


Fig. 1. Octahedron position of cations B in pyrochlores.

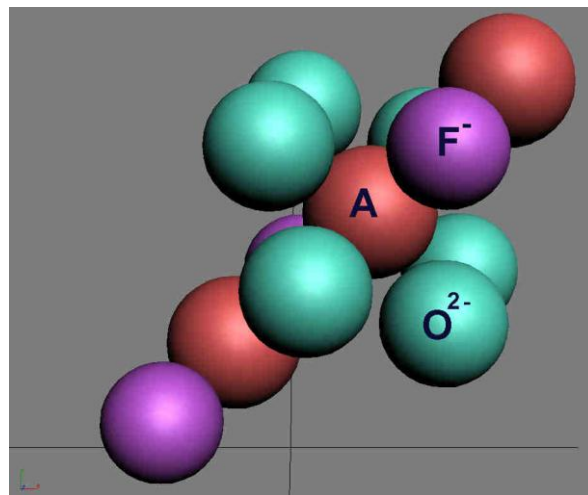


Fig. 2. Polyhedron position of cations A in pyrochlores.

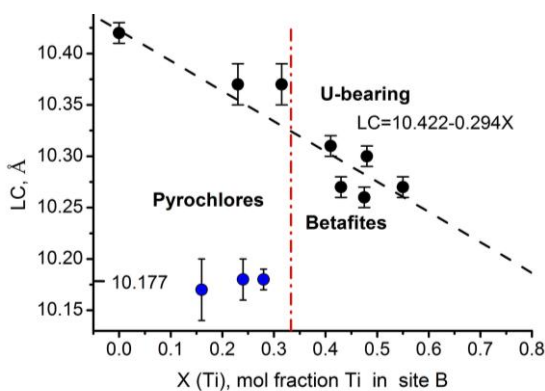


Fig. 3-a

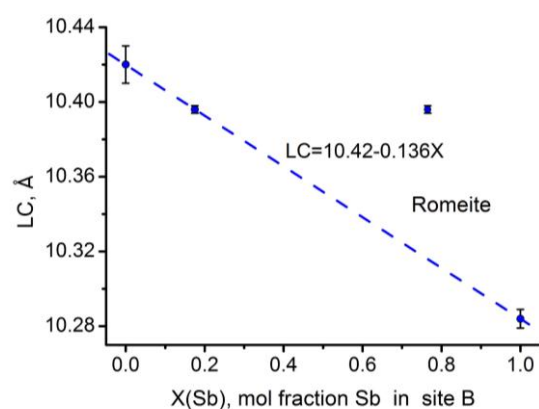


Fig. 3-b

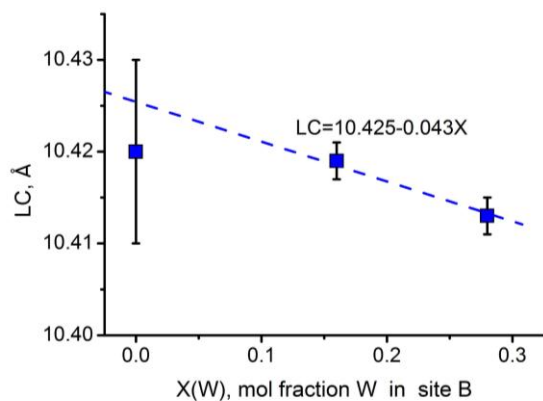


Fig. 3-c

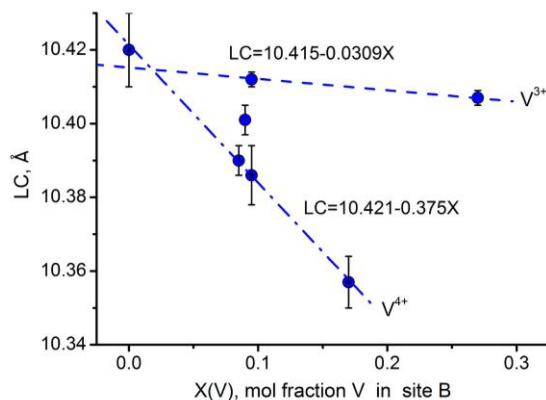


Fig. 3-e

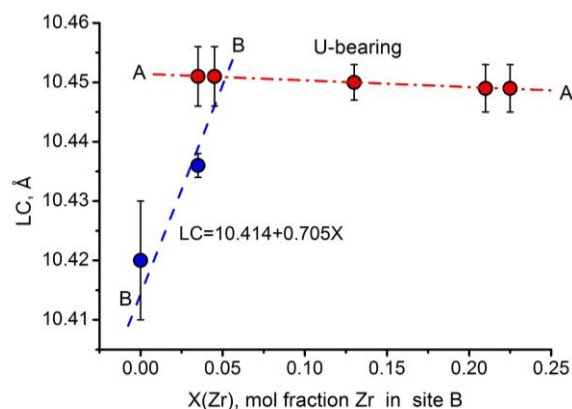


Fig. 3-d

Fig. 3 (a-e). The influence of mol fraction and nature of cation in B position on lattice constant (LC) of pyrochlores by experimental data

Table 1. Crystal radii of ions [Shannon, 1976]

| Ion | R _{cr} , Å | | |
|------------------|---------------------|-------|------|
| | CN=2 | CN=6 | CN=8 |
| O ²⁻ | 1.21 | – | – |
| F ⁻ | 1.145 | – | – |
| OH ⁻ | 1.18 | – | – |
| Nb ³⁺ | – | 0.78 | – |
| Ta ³⁺ | – | 0.78 | – |
| Ti ⁴⁺ | – | 0.745 | – |
| Sb ⁵⁺ | – | 0.74 | – |
| W ³⁺ | – | 0.76 | – |
| W ⁶⁺ | – | 0.74 | – |
| Zr ⁴⁺ | – | 0.86 | – |
| V ³⁺ | – | 0.78 | – |
| V ⁴⁺ | – | 0.72 | 0.86 |
| V ⁵⁺ | – | 0.68 | – |
| U ⁶⁺ | – | 0.87 | – |
| U ³⁺ | – | 0.90 | – |
| U ⁴⁺ | – | 1.03 | 1.14 |
| Na ⁺ | – | – | 1.32 |
| Ca ²⁺ | – | – | 1.26 |
| K ⁺ | – | – | 1.65 |

Each A cation is surrounded by six O²⁻ and two Y anions (in our case by F⁻) forming cubic polyhedron (Fig. 2). The Y anions form a broken line with A cations. The A-Y and A-O bond in cubic polyhedron must be ionic. For ideal pyrochlore (NaCa)Nb₂O₆F, the contrary, R_{Ca-F} > R_{Ca} + R_F and thus it has a chance of small and big cations for substitution in A position.

In this study, we considered the influence of crystal dimensions of cations and anions (O²⁻, F⁻) on lattice constants of Na, Ca, U, Nb, Ta, Ti, Sb, Zr, V, and W - bearing pyrochlores obtained by hydrothermal synthesis. Pyrochlores synthesis was performed in Pt capsules on a hydrothermal line at T = 800°C, P = 200 MPa and fO₂ maintained with Co-CoO, Fe₂O₃-Fe₃O₄, and Cu₂O-CuO buffers. The thorough grinding mixtures of NaF (or Na₂CO₃), CaCO₃, Nb₂O₅, Ta₂O₅, TiO₂, ZrO₂, V₂O₅, U₃O₈, and UO₄×2H₂O chemicals were the starting materials. The medium for the synthesis was the saturated at 22°C NaF solution (≈1 mol/kg H₂O)

According to the informative card and atomic positions of cations and anions in it, a lattice constant of ideal pyrochlore corresponds to equation

$$a_0 = 8 \times (R_B + k \times R_{O_2}) \times \cos 45^\circ = 8 \times (R_A + l \times R_F) \times \cos 45^\circ$$

or

$$a_0 = 5.657 \times (R_B + k \times R_{O_2}) = 5.657 \times (R_A + l \times R_F) \quad (1).$$

If cations involving in octahedron position B define LC, then the right part of equation 1 is defined by left part

Abstracts

of the equation. In case, when cations from table 1 substitute for cation Nb^{5+} (or Ta^{5+}) in B position, the equation 1 assumes a form:

$$a_0 = 5.657 \times (R_{Nb} (1 - X_B) + X_B \times R_{B \neq Nb} + k \times R_{O_2}) \quad (2)$$

The substitution of the corresponding radii (table 1) and the dependences of LC from mol fraction of cation (Fig. 3 a-e) is shown

| | |
|---|--|
| for Sb^{5+} bearing pyrochlores | $k = 0.878 - 0.0132 \times X_{Sb}$; |
| W^{5+} $k = 0.878 + 0.0102 \times X_{W^{5+}}$ or W^{6+} | $k = 0.878 + 0.0267 \times X_{W^{6+}}$; |
| Ti^{4+} $k = 0.878 - 0.03053 \times X_{Ti^{4+}}$; | |
| V^{4+} $k = 0.878 - 0.00526 \times X_{V^{4+}}$ and V^{3+} | $k = 0.878 - 0.0309 \times X_{V^{3+}}$. |

The data obtained show that k coefficient in Eq. 2 depends although weakly on mole fraction of substitutive cation. The k coefficient can be accepted as constant, $k = 0.878$ for the pyrochlores where were replaced less 0.5 mol of Nb^{5+} (or Ta^{5+}). In this case the calculated value of LC will be in within the error ($\pm 0.02 \text{ \AA}$) corresponds to the value founded by X-ray methods.

Thus, the correlation close to linear between LC of pyrochlore, mole fraction and crystal radii of cation substitute for B position is found.

The authors are grateful to A.N. Nekrasov, O.L. Samokhvalova, and T.N. Dokina for research assistance. Financial support by RFBR, project 11-05-01185-a and ONZ program N2.

References :

1. Atencio D., M.B. Andrade, A.G. Christy et al. (2010). The pyrochlores supergroup of minerals: nomenclature. *The Canad. Mineral.*, v.48, p. 673-698.
2. Chakoumakos B.C. (1984). Systematics of the Pyrochlore Structure Type, Ideal $A_2B_2X_6Y$. *J. Solid State Chem.*, v. 53, p. 120-129.
3. Hogarth D.D. (1977). Classification and nomenclature of the pyrochlore group. *Amer. Min.*, v. 62, p. 403-410.
4. Shannon R.D. (1976). Revised effective ionic radii and systematic studies of interatomic distances in halides and chalcogenides. *Acta Cryst.*, A32, p. 751-767

Stolyarova T.A., Osadchy E G. Enthalpy of formation of platinum monobismuthide from elements

Institute of Experimental Mineralogy RAS, Chernogolovka

Abstract The work dedicated to platinum monobismuthide. It is described the method of the synthesis PtBi. The reaction of bismuthide platinum was used for thermochemical studies. Calorimetric measurements were conducted on a high-temperature vacuum-blocking calorimetric system. The values was obtained: for PtBi:

$$\Delta_f H_{298,15K}^0 = -29.50 \pm 0.41 \text{ kJ/mol}$$

Key words: bismuthide platinum, enthalpy, thermochemistry, calorimetry.

Citation: Stolyarova T.A., E G.Osadchy (2013). Enthalpy of formation of platinum monobismuthide from elements.

Binary intermetallic compounds of platinum and palladium are encountered as minerals in the series of the later stages of formation of magmatogenic sulfide deposits rich in platinum group elements. Native metals and simple binary intermetallic compounds govern physical-chemical confines of the lower limit of oxide and chalcogenide ore formation.

Thermodynamic properties of most intermetallic compounds are still unknown. That disables physical-chemical analysis of the parageneses, which is the basic matter for understanding the geochemical peculiarities of ore formation processes. Platinum bismuthide was chosen as the object of investigation.

Preliminary investigations showed that the synthesis of platinum monobismuthide from elements (powder platinum of 99.99% purity and powdered bismuth of HP grade) in vacuum quartz geass ampoule took place at 700°C for several minutes (5-7). The reaction $Pt+Bi=PtBi$ has been studied.

Calorimetric determinations were carried out on the high temperature vacuum-blocking calorimeter made in the laboratory of mineral thermodynamics in IEM RAS, which had been described earlier [Soboleva., Vasil'ev, 1962, Fleisher., Stolyarova, 1968]. An ampoule with a sample was placed into a resistance furnace inside a calorimetric bomb, which was further filled with argon under a pressure of about 5 atm. The vessel with the calorimetric bomb was evacuated until residual pressure equaled 10-2 mm mer.col. Isometric cover temperature was 25+0.02oC. Electric energy was measured accurate to 0.02%. Temperature rise in the course of experiment was fixed by a copper resistance thermometer (~865 ohm at 25oC), located along the calorimetric bomb. The calorimeter was preliminarily calibrated with electric energy. The accuracy of determination of heat value was 0.005%. Synthesis reactions within the calorimeter were completed during the first heating (5-7 minutes). Repeated heating had no additional effect, which validated that the reaction had been completed in full during the first experiment.

X-ray phase analysis of the products of calorimetric experiments confirmed the presence of only given compounds.

The results of calorimetric investigations are given in Table 1.

Mean-square error was calculated at the significance level of 95% [Nalimov, 1960]. The following value was obtained for reaction 1:

$$\Delta_f H_{298,15K}^0 = -29.5 + 0.41 \text{ kJ/mol.}$$

The work has been done with the financial support of the program "Leading scientific schools", grant HIII-5877.2012.5, the program ONZ N 2 and RFBR, grant 12-05-01005.

References:

1. Fleisher L.L., T.A. Stolyarova (1978). Automatization of the process of measurement of electric energy of high-temperature calorimetric vessel. *Measur. Technique*, N2, p.60.
2. Nalimov V.V. (1960). The use of mathematics statistics at substance analysis, M: Nauka
3. Soboleva M.S., L.V. Vasil'ev (1962). Enthalpy of-formation of Ni tellurides никеля $NiTe_{1.00}$ - $NiTe_{1.5}$. *Vestn. Leningrad Univ. Ser. physics and chemistry*, v I 6, - p.153.

Table 1. Enthalpy of formation of PtBi from elements, mm 404,058.

| Run No. | Weight, g | Operation conditions of furnace | | | | |
|---------|-----------|---------------------------------|--------|--|--|---|
| | | t(s) | V(V) | J(A) at the moment of switching off, A | $\int_{t_0}^{t_k} Idt$ by apparatus, (A·s) | $\int_{t_0}^{t_k} Idt$ in experiment (A·s)к |
| 1 | 3.7296 | 361.363 | 38.227 | 3.272 | 1195.895 | 1198.683 |
| 2 | 3.0658 | 360.1 18 | 38.229 | 3.265 | 1188.489 | 1188.512 |
| 3 | 2.8446 | 361.410 | 38.182 | 3.268 | 1191.373 | 1192.348 |
| 4 | 4.0753 | 360.808 | 38.218 | 3.275 | 1192.390 | 1194.673 |
| 5 | 2.4011 | 364.721 | 38.217 | 3.269 | 1204.867 | 1206.857 |
| 6 | 2.9914 | 360.095 | 38.210 | 3.266 | 1186.774 | 1186.719 |
| 7 | 1.8415 | 360.642 | 39.108 | 3.418 | 1241.958 | 1243.790 |

End Table 1.

| Run No. | Rate of cooling 10^{-5} (K·min) | $\Delta R + \delta$, Ω | Amount of heat in experiment, Q(J) | | | $\Delta H_{298,15K}^0$ (kJ·mol ⁻¹) in individual run |
|---------|-----------------------------------|--------------------------------|------------------------------------|-----------|-------------|--|
| | | | total | on heater | in reaction | |
| 1 | 33 | 6.9679 | 46089.2 | 45822.1 | 267.1 | -28.94 |
| 2 | 34 | 6.9029 | 45659.2 | 45435.6 | 223.6 | -29.47 |
| 3 | 37 | 6.9171 | 45453.2 | 45526.2 | 227.0 | -32.24 |
| 4 | 36 | 6.9452 | 45939.0 | 45658.0 | 281.0 | -27.86 |
| 5 | 39 | 6.9994 | 46297.5 | 46122.4 | 175.1 | -29.47 |
| 6 | 43 | 6.9165 | 45558.3 | 45344.5 | 213.8 | -28.88 |
| 7 | 40 | 7.4050 | 48776.0 | 48642.1 | 133.9 | -29.39 |
| Average | | | | | | -29.46±0.41 |

Note: $\Delta R + \delta$ - change of the thermometer resistance with the correction for heat exchange

1-5 experiments- heat value of the calorimeter $W = 6614.5 \pm 2$ J/Ω. 6-7 - $W = 6586.9 \pm 2$ J/Ω;

Shornikov S. I. Thermodynamic properties of the K_2O - GeO_2 melts

V. I. Vernadsky Institute of Geochemistry and Analytical Chemistry RAS, Moscow

Abstract. Within the framework of the developed semi-empirical model based on the theory of ideal associated solutions, the thermodynamic properties of the K_2O - GeO_2 melts were calculated in the temperature region 600–1600 K. The results of calculations are compared with available experimental information.

Key words: thermodynamic properties of oxide melts, the K_2O - GeO_2 system.

Citation: Shornikov, S. I. (2013), Thermodynamic properties of the K_2O - GeO_2 melts. *Vestn. Otd. nauk Zemle*, 4, (doi:).

Physico-chemical properties of potassium germanates and melts in the K_2O - GeO_2 system are of interest to a theoretical calculations of low-temperature analog of the K_2O - SiO_2 system, which important in the geochemical

Abstracts

researches and due to their practical application in technics. The available information on structure and properties of the compounds and the phase relations in considered system is poor [Schwarz & Heinrich, 1932;

Gutkina et al., 1984], the version of the phase diagram is presented in fig. 1.

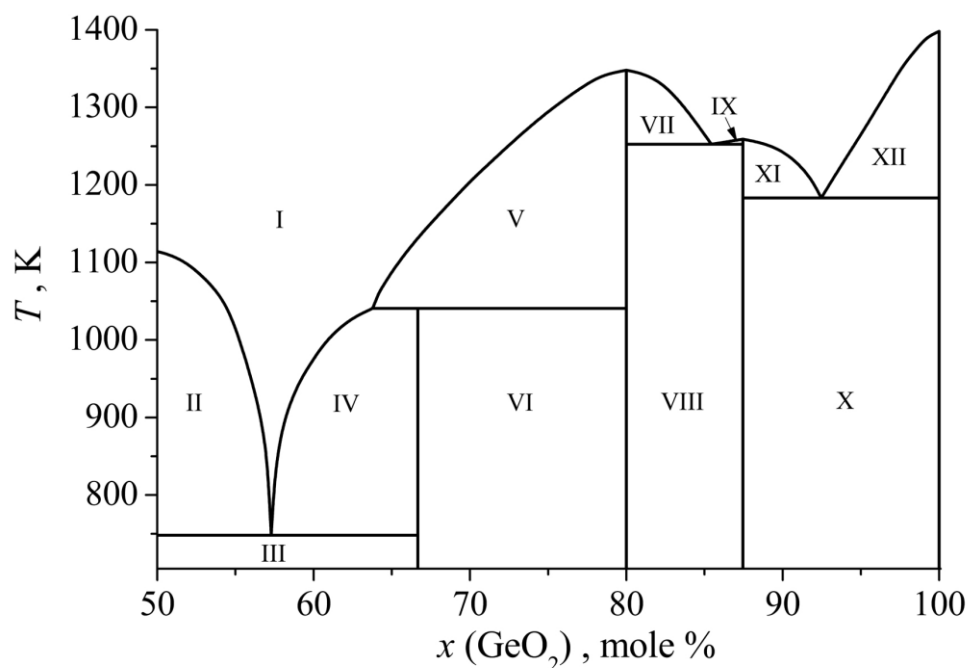


Fig. 1. The phase diagram of the K_2O-GeO_2 system [Schwarz & Heinrich, 1932; Gutkina et al., 1984]. Table of symbols: I – liquid; II – K_2GeO_3 + liquid; III – K_2GeO_3 + $K_2Ge_2O_5$; IV – $K_2Ge_2O_5$ + liquid; V and VII – $K_2Ge_4O_9$ + liquid; VI – $K_2Ge_2O_5$ + $K_2Ge_4O_9$; VIII – $K_2Ge_4O_9$ + $K_2Ge_7O_{15}$; IX and XI – $K_2Ge_7O_{15}$ + liquid; X – $K_2Ge_7O_{15}$ + GeO_2 ; XII – GeO_2 + liquid.

Table 1. The enthalpies (ΔH_T) and the entropies (ΔS_T) of formation of potassium germanates from the simple oxides [Kozhina et al., 1999; Bessedina et al., 2002; Shornikov, 2005].

| Compound | T, K | $\Delta H_T,$ kJ/mole | $\Delta S_T,$ J / (mole · K) | Reference |
|-----------------|-----------|--------------------------|---------------------------------|--------------------------|
| K_2GeO_3 | 1114–1550 | -134.2 ± 1.5 | 12.4 ± 1.5 | [Shornikov, 2005] |
| – " – | 1223 | -171.7 ± 2.5 | -45.7 ± 2.5 | [Kozhina et al., 1999] |
| $K_2Ge_2O_5$ | 298 | -113.9 ± 2.5 | – | [Bessedina et al., 2002] |
| – " – | 1140–1550 | -98.3 ± 1.5 | 11.3 ± 1.5 | [Shornikov, 2005] |
| – " – | 1223 | -136.0 ± 2.5 | -43.6 ± 2.5 | [Kozhina et al., 1999] |
| $K_2Ge_4O_9$ | 298 | -80.1 ± 2.5 | – | [Bessedina et al., 2002] |
| – " – | 1223 | -95.2 ± 2.5 | -37.2 ± 2.5 | [Kozhina et al., 1999] |
| – " – | 1348–1550 | -63.5 ± 1.5 | 8.3 ± 1.5 | [Shornikov, 2005] |
| $K_2Ge_7O_{15}$ | 298 | -56.3 ± 2.5 | – | [Bessedina et al., 2002] |
| – " – | 1223 | -64.4 ± 2.5 | -24.3 ± 2.5 | [Kozhina et al., 1999] |
| – " – | 1253–1550 | -41.7 ± 1.5 | 5.7 ± 1.0 | [Shornikov, 2005] |

Hydrothermal equilibria ...

Table 2. The Gibbs energy of formation from elements of condensed phases and vapor species over the K_2O-GeO_2 system at 1500 K, calculated in the present study according to data [Glushko et al., 1978–1982; Shornikov & Archakov, 1999; Kozhina et al., 1999; Bessedina et al., 2002; Shornikov, 2005].

| Condensed phases | | | Gas phase | | |
|------------------|-------------------------------------|-----------------|-------------------------------------|---------------|-------------------------------------|
| Solid phases | $\Delta_f G^\circ_{1500}$, kJ/mole | Liquid phases | $\Delta_f G^\circ_{1500}$, kJ/mole | Vapor species | $\Delta_f G^\circ_{1500}$, kJ/mole |
| K_2O | -161.387 | K_2O | -174.367 | K | -33.956 |
| K_2GeO_3 | -729.395 | K_2GeO_3 | -757.684 | K_2 | -2.918 |
| $K_2Ge_2O_5$ | -1062.240 | | | KO | -25.891 |
| $K_2Ge_4O_9$ | -1698.054 | $K_2Ge_4O_9$ | -1704.042 | K_2O | -113.676 |
| $K_2Ge_7O_{15}$ | -2559.612 | $K_2Ge_7O_{15}$ | -2572.559 | K_2O_2 | -111.814 |
| GeO_2 | -290.807 | GeO_2 | -292.357 | Ge | 170.658 |
| | | | | Ge_2 | 221.010 |
| | | | | GeO | -155.217 |
| | | | | GeO_2 | -101.526 |
| | | | | Ge_2O_2 | -295.507 |
| | | | | Ge_3O_3 | -378.763 |
| | | | | O | 154.920 |
| | | | | O_2 | 0.000 |
| | | | | O_3 | 243.150 |

This investigation presents the calculation of thermodynamic properties of the K_2O-GeO_2 melts at temperatures from 600 to 1600 K within framework of the ideal associated solutions theory. The simplified lattice model, as before for the $CaO-MgO-Al_2O_3-SiO_2$ systems [Shornikov, 2009], accounts for the intermolecular interactions using the semi-phenomenological parameters, which were determined on the base of the experimental [Shornikov & Archakov, 1999; Kozhina et al., 1999; Bessedina et al., 2002; Shornikov, 2005] and reference [Glushko et al., 1978–1982] thermodynamic data, presented in the table 1. The initial thermodynamic data considered 11 condensed phases (6 solid and 5 liquid) and 14 gas species, these components are listed in the table 2.

The same table 2 gives the calculated values of the Gibbs energies of formation from elements ($\Delta_f G^\circ_T$) for the

compounds and the vapor species over the K_2O-GeO_2 system. They were used for the calculation of the equilibrium conditions in the system at a given composition and temperature. The required equation solution for the total Gibbs energy for the system studied was found by the widely used approach, namely the Gibbs energy minimization method. The oxide activities $a(i)$ and the mixing in the K_2O-GeO_2 melts (ΔG_T) are represented in fig. 2 and 3 in comparison to experimental data [Shornikov & Archakov, 1999; Kozhina et al., 1999; Shornikov, 2005].

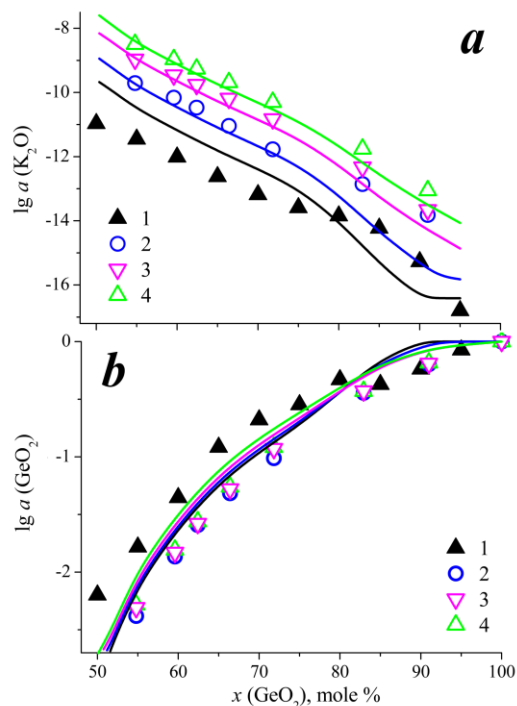
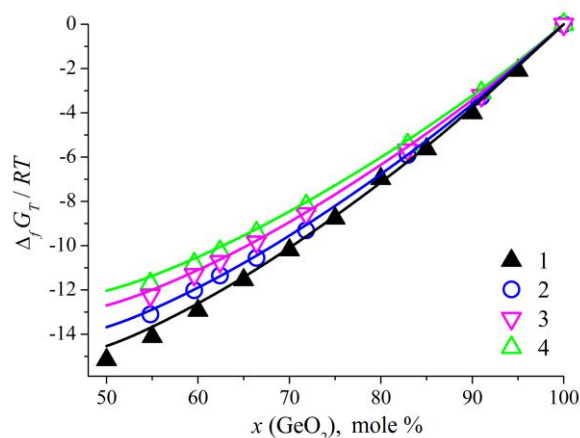


Fig. 2. The activities of K_2O (a) and GeO_2 (b) in the K_2O-GeO_2 melts: 1 – obtained by the e. m. f method at 1223 K [Kozhina et al., 1999], 2–4 – obtained by Knudsen effusion mass spectrometric method at 1300, 1400 and 1473 K [Shornikov & Archakov, 1999; Shornikov, 2005]; and calculated in the present study according to semi-empirical model at the same temperatures, represented by lines of the same color.



We can see in fig. 2 that the K_2O and GeO_2 activities in the K_2O – GeO_2 melts calculated in the present study corresponded satisfactory to experimental data [Shornikov & Archakov, 1999; Kozhina et al., 1999; Shornikov, 2005], showing their increase with temperature growth. Higher values of the GeO_2 activities (fig. 2b) calculated by Kozhina et al. [Kozhina et al., 1999] using the K_2O activities obtained by the e. m. f method at temperature of 1223 K [Kozhina et al., 1999] probably were caused by procedure of renormalizing the chemical potential values of the second component. It can lead also to large errors in the melt entropies ΔS_T (table 1).

We may observe also on fig. 2a the differences increasing between the K_2O activities calculated in the present study from the same obtained by Knudsen effusion mass spectrometric method at temperature of 1300 K [Shornikov & Archakov, 1999] in the range of K_2O low concentration. Probably it is caused by their possible error. However these deviations have not been influenced on the values of mixing energy of the K_2O – GeO_2 melts (fig. 3).

Thus, within the framework of the developed semi-empirical model based on the theory of ideal associated solution [Shornikov, 2009], the thermodynamic properties of the K_2O – GeO_2 melts were calculated in the temperature range of 600–1600 K. The calculation results are corresponding to available experimental data [Shornikov & Archakov, 1999; Kozhina et al., 1999; Bessedina et al., 2002; Shornikov, 2005]. They also can be used as for theoretical calculations of thermodynamic properties of multicomponent melts containing this system compounds and in the practical purposes.

References:

- Bessedina, S. A., V. G. Konakov, M. M. Schultz (2002). Acid-base properties of melts of the M_2O – GeO_2 system ($M = Li, Na, K$), *Rev. Adv. Mater. Sci.*, vol. 3, no. 1 pp. 37–66.
- Glushko, V. P., L. V. Gurvich, G. A. Bergman, I. V. Veitz, V. A. Medvedev, G. A. Khachkuruzov, V. S. Youngman (1978–1982). Thermodynamic properties of individual substances, M.: Nauka.
- Gutkina, N. G., A. I. Ignatiev, I. I. Kozhina, E. E. Shalamaiko (1984). Glassforming, glass properties and crystallization in systems on a basis K_2O , TiO_2 and GeO_2 , *Russ. Phys. Chem. Glasses*, v. 10, no. 5, pp. 534–540.
- Kozhina, E. L., S. A. Bessedina, V. G. Konakov, M. M. Shultz (1999). A study of thermodynamic

Fig. 3. The mixing energy in the K_2O – GeO_2 melts: 1 – obtained by the e. m. f method at 1223 K [Kozhina et al., 1999], 2–4 – obtained by Knudsen effusion mass spectrometric method at 1300, 1400 and 1473 K [Shornikov & Archakov, 1999; Shornikov, 2005]; and calculated in the present study according to semi-empirical model at the same temperatures, represented by lines of the same color.

properties of the K_2O – GeO_2 system by the e. m. f method, *Russ. Phys. Chem. Glasses*, v. 25, no. 5, pp. 529–537.

- Schwarz, R., F. Heinrich (1932). Contributions to chemistry of germanium: IX. Germanates of the alkali and alkali-earth metals, *Z. anorg. allg. Chem.*, vol. 205, no. 1, pp. 43–48.
- Shornikov, S. I., I. Yu. Archakov (1999). Mass spectrometric study of vaporization processes and thermodynamic properties of the K_2O – GeO_2 system, Proc. 5th ESG Conf. *Glass and technology for the 21st century*. Prague: The Czech Glass Society, CD-ROM.
- Shornikov, S. I. (2005). Vaporization behavior and thermodynamic properties of K_2O – GeO_2 melts studied by mass spectrometry, *Russ. Inorg. Mater.*, v. 41, no. 12, pp. 1345–1356.
- Shornikov, S. I. (2009). Investigation of abilities of thermodynamic approaches on calculations of oxide activities in the compounds of the CaO – MgO – Al_2O_3 – SiO_2 system, *Vestnik Otdelenia nauk o Zemle RAN*, vol. 27, no. 1, <http://onznnews.wdcb.ru/publications/asempg/planet-33.pdf>.

Shornikov S. I. Thermodynamic properties of K_2O – SiO_2 melts

V. I. Vernadsky Institute of Geochemistry and Analytical Chemistry RAS, Moscow

Abstract. Within the framework of the developed semi-empirical model, the thermodynamic properties of the K_2O – SiO_2 melts were calculated in the temperature region 800–1800 K. The calculated values of the oxide activities and the mixing energies of potassium silicate melts are compared with available experimental information.

Key words: thermodynamic properties of oxide melts, the K_2O – SiO_2 system.

Citation: Shornikov, S. I. (2013), Thermodynamic properties of the K_2O – SiO_2 melts. *Vestn. Otd. nauk Zemle*, 4, (doi:).

Physico-chemical properties of potassium silicates and melts in the K_2O – SiO_2 system are of interest to a theoretical calculations in the petrological and geochemical researches and due to their practical application in technics. In spite of numerous investigations [Glushko et al., 1978–1982], the thermodynamic properties of these compounds are contradictory that was considered earlier [Shornikov, 2005]. The phase diagram presented in the fig. 1 [Kracek et al., 1937].

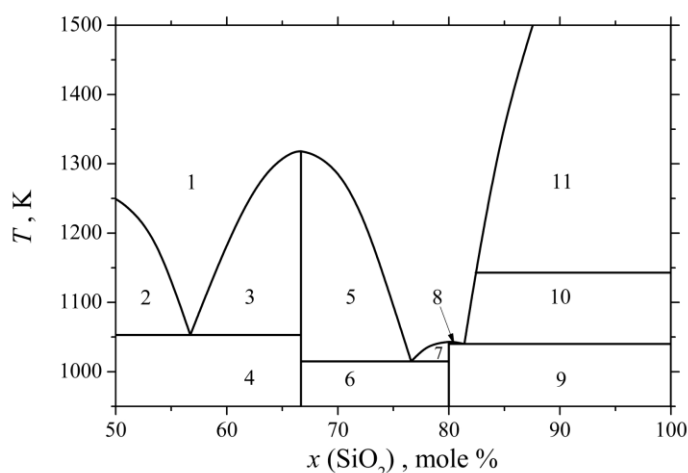


Fig. 1. The phase diagram of the K_2O-SiO_2 system [Kracek et al., 1937].
Table of symbols: 1 – liquid; 2 – K_2SiO_3 + liquid; 3, 5 – $K_2Si_2O_5$ + liquid; 4 – K_2SiO_3 + $K_2Si_2O_5$; 6 – $K_2Si_2O_5$ + $K_2Si_4O_9$; 7, 8 – $K_2Si_4O_9$ + liquid; 9. – $K_2Si_4O_9$ + SiO_2 (quartz) + liquid; 10 – SiO_2 (quartz) + SiO_2 (tridymite) + liquid; 11 – SiO_2 (tridymite) + SiO_2 (cristobalite) + liquid.

This investigation presents the calculation of thermodynamic properties of the K_2O-SiO_2 melts at temperatures from 800 to 1800 K within framework of the ideal associated solutions theory. The simplified lattice model, as before for the $CaO-MgO-Al_2O_3-SiO_2$ systems [Shornikov, 2009], accounts for the intermolecular interactions using the semi-phenomenological parameters. They were determined on the base of the experimental [Kozhina, 1990; Borisova & Ushakov, 1998; Zaitsev et al., 2000] and reference [Glushko et al., 1978–1982; Barin et al., 1993; Chase, 1998] thermodynamic data, presented in the table 1 and 2.

The initial thermodynamic data considered 12 condensed phases (6 solid and 6 liquid) and 14 gas species, these components are listed in the table 3. The same table 3 gives the calculated values of the Gibbs energies of formation from elements ($\Delta_f G^\circ_T$) for the compounds and the vapor species over the K_2O-SiO_2

system. They were used for the calculation of the equilibrium conditions in the system at a given composition and temperature. The required equation solution for the total Gibbs energy for the system studied was found by the widely used approach, namely the Gibbs energy minimization method.

According to fig. 2 and 3, the calculated values of oxide activities $a(i)$ and mixing energies (ΔG_T) of the K_2O-SiO_2 melts are well correspond to the experimental data [Kozhina, 1990; Zaitsev et al., 2000]. The results of Kozhina [Kozhina, 1990] obtained at the temperature of 973 K not considered as they correspond to homogeneous area that contradicts to the phase relations represented on the fig. 1. At the same time the mixing energy values are close to the calculated in the present study in this case (fig. 3).

Table 1. The enthalpies (ΔH_T) and the entropies (ΔS_T) of formation of potassium silicates from the simple oxides [Kozhina, 1990; Barin et al., 1993; Borisova & Ushakov, 1998; Zaitsev et al., 2000; Shornikov, 2005].

| Compound | T, K | ΔH_T , kJ/mole | ΔS_T , J / (mole · K) | Reference |
|--------------|-----------|---------------------------|----------------------------------|----------------------------|
| K_2SiO_3 | 879–1050 | -145.94±0.57 | 5.24±0.57 | [Zaitsev et al., 2000] |
| – " – | 973 | -144.20±4.60 | -5.44±2.93 | [Kozhina, 1990] |
| – " – | 973 | -145.80±4.50 | – | [Borisova & Ushakov, 1998] |
| – " – | 1000–1249 | -148.02±0.72 | -7.59±0.65 | [Barin et al., 1993] |
| – " – | 1249–1800 | -123.86±0.01 | 11.68±0.01 | [Barin et al., 1993] |
| – " – | 1249–1730 | -159.66±1.03 | -17.85±0.74 | [Zaitsev et al., 2000] |
| – " – | 1249–1800 | -137.15 | 12.28 | [Shornikov, 2005] |
| – " – | 1273 | -144.79±4.60 | -0.84±2.93 | [Kozhina, 1990] |
| $K_2Si_2O_5$ | 869–1014 | -112.56±0.54 | 3.47±0.50 | [Zaitsev et al., 2000] |
| – " – | 973 | -109.27±4.60 | -0.46±2.93 | [Kozhina, 1990] |
| – " – | 973 | -101.60±2.50 | – | [Borisova & Ushakov, 1998] |
| – " – | 1000–1318 | -113.48±0.19 | -3.83±0.16 | [Barin et al., 1993] |
| – " – | 1273 | -99.11±4.60 | 6.49±2.93 | [Kozhina, 1990] |
| – " – | 1318–1800 | -97.23±0.12 | 8.47±0.07 | [Barin et al., 1993] |
| – " – | 1318–1730 | -117.59±0.51 | -8.36±0.35 | [Zaitsev et al., 2000] |
| – " – | 1318–1800 | -101.89 | 11.57 | [Shornikov, 2005] |
| $K_2Si_4O_9$ | 800–1041 | -60.45±0.25 | 3.38±0.28 | [Barin et al., 1993] |
| – " – | 891–1041 | -64.90±0.50 | -1.18±0.41 | [Zaitsev et al., 2000] |
| – " – | 973 | -62.45±4.60 | 3.85±2.93 | [Kozhina, 1990] |
| – " – | 973 | -61.40±2.20 | – | [Borisova & Ushakov, 1998] |
| – " – | 1043–1800 | -55.59±0.32 | 7.99±0.22 | [Barin et al., 1993] |
| – " – | 1050–1730 | -70.01±0.29 | -1.75±0.21 | [Zaitsev et al., 2000] |
| – " – | 1273 | -57.00±4.60 | 7.62±2.93 | [Kozhina, 1990] |

Abstracts

Table 2. The temperatures (T_m), the enthalpies (ΔH_m) and entropies (ΔS_m) of melting of potassium silicates [Takahashi & Yoshio, 1970; Glushko et al., 1978–1982; Barin et al., 1993; Chase, 1998; Bale et al., 2002].

| Compound | T_m , K | ΔH_T , kJ/mole | ΔS_T , J / (mole · K) | Reference |
|---|-----------|---------------------------|----------------------------------|-----------------------------|
| K ₂ O | 1013±10 | 27.00±3.00 | 26.65±2.96 | [Glushko et al., 1978–1982] |
| – " – | 1013 | 27.20±1.50 | 26.85±1.50 | [Barin et al., 1993] |
| K ₂ SiO ₃ | 1249 | 5.50±3.00 | 4.40±2.40 | [Takahashi & Yoshio, 1970] |
| – " – | 1249±2 | 10.00±5.00 | 8.01±4.00 | [Glushko et al., 1978–1982] |
| – " – | 1249 | 25.10±1.50 | 20.10±1.20 | [Barin et al., 1993] |
| – " – | 1249 | 25.10±6.28 | 20.10±5.02 | [Chase, 1998] |
| – " – | 1250 | 7.44±1.50 | 5.95±1.20 | [Bale et al., 2002] |
| K ₂ Si ₂ O ₅ | 1318 | 10.60±1.00 | 8.04±0.76 | [Takahashi & Yoshio, 1970] |
| – " – | 1318±5 | 11.73±0.33 | 8.90±0.25 | [Glushko et al., 1978–1982] |
| – " – | 1318 | 13.67±1.50 | 10.37±1.13 | [Barin et al., 1993] |
| – " – | 1319 | 15.82±1.50 | 11.99±1.13 | [Bale et al., 2002] |
| K ₂ Si ₄ O ₉ | 1043±10 | 9.79±1.50 | 9.39±1.50 | [Barin et al., 1993] |
| – " – | 1044 | 6.88±1.50 | 6.59±1.50 | [Bale et al., 2002] |
| SiO ₂ | 1996±5 | 9.80±0.50 | 4.81±0.50 | [Glushko et al., 1978–1982] |
| – " – | 1996 | 9.57±0.50 | 4.79±0.50 | [Barin et al., 1993] |

Table 3. The Gibbs energy of formation from elements of condensed phases and vapor species over the K₂O–SiO₂ system at 1500 K, calculated in the present study according to data [Glushko et al., 1978–1982; Kozhina, 1990; Zaitsev et al., 2000].

| Solid phases | Condensed phases | | Gas phase | | |
|---|--|---|--|--------------------------------|--|
| | $\Delta_f G^\circ_{1500}$, kJ/mole | Liquid phases | $\Delta_f G^\circ_{1500}$, kJ/mole | Vapor species | $\Delta_f G^\circ_{1500}$, kJ/mole |
| K ₂ O | -161.387 | K ₂ O | -174.367 | K | -33.956 |
| K ₄ SiO ₄ | -1399.608 | K ₄ SiO ₄ | -1420.342 | K ₂ | -2.918 |
| K ₂ SiO ₃ | -1089.318 | K ₂ SiO ₃ | -1099.514 | KO | -25.891 |
| K ₂ Si ₂ O ₅ | -1769.285 | K ₂ Si ₂ O ₅ | -1776.017 | K ₂ O | -113.676 |
| K ₂ Si ₄ O ₉ | -3077.325 | K ₂ Si ₄ O ₉ | -3086.088 | K ₂ O ₂ | -111.814 |
| SiO ₂ | -649.708 | SiO ₂ | -644.903 | Si | 229.272 |
| | | | | Si ₂ | 286.080 |
| | | | | Si ₃ | 332.834 |
| | | | | SiO | -225.709 |
| | | | | SiO ₂ | -324.873 |
| | | | | Si ₂ O ₂ | -620.459 |
| | | | | O | 154.920 |
| | | | | O ₂ | 0.000 |
| | | | | O ₃ | 243.150 |

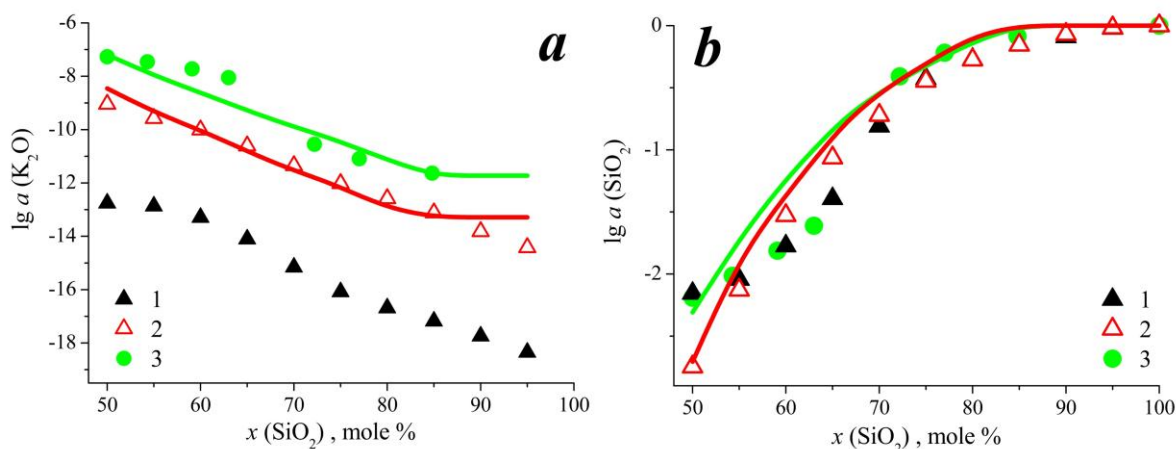


Fig. 2. The activities of K₂O (a) and SiO₂ (b) in the K₂O–SiO₂ melts: 1, 2 – obtained by the e. m. f method at 973 and 1273 K [Kozhina, 1990], 3 – obtained by Knudsen effusion mass spectrometric method at 1473 K [Zaitsev et al., 2000]; and calculated in the present study according to semi-empirical model at the same temperatures, represented by lines of the same color.

Thus, within the framework of the developed semi-empirical model based on the theory of ideal associated solution [Shornikov, 2009], the thermodynamic properties of the K_2O-SiO_2 melts were calculated in the temperature range of 800–1800 K. The calculation results are corresponding to available experimental data [Kozhina, 1990; Zaitsev et al., 2000]. They also can be used as for theoretical calculations of thermodynamic properties of multicomponent melts containing this system compounds and in the practical purposes.

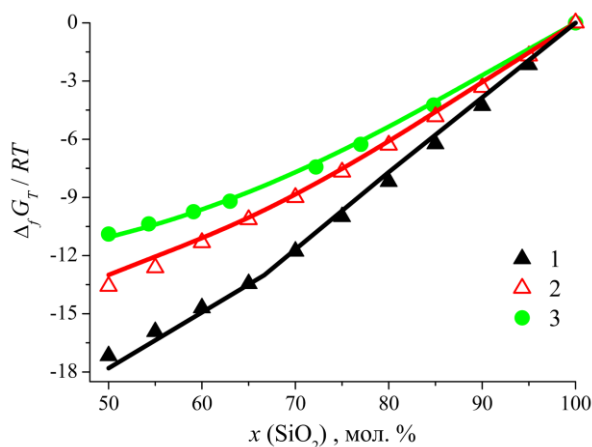


Fig. 3. The mixing energy in the K_2O-SiO_2 melts: 1, 2 – obtained by the e. m. f method at 973 and 1273 K [Kozhina, 1990], 3 – obtained by Knudsen effusion mass spectrometric method at 1473 K [Zaitsev et al., 2000]; and calculated in the present study according to semi-empirical model at the same temperatures, represented by lines of the same color.

References:

- Bale, C. W., P. Chartrand, S. A. Degterov, G. Eriksson, K. Hack, R. Ben Mahfoud, J. Melancon, A. D. Pelton, S. Petersen (2002). FactSage thermochemical software and databases, *CALPHAD*, vol. 26, no. 2, pp. 189–228.
- Barin, I., F. Sauert, E. Schultze-Rhonhof, W. C. Sheng (1993). Thermochemical data of pure substances, Weinheim: VCH, 1739 pp.
- Borisova, N. V., V. M. Ushakov (1998). High-temperature calorimetry of glasses and crystals in the K_2O-SiO_2 system, *Russ. Glass & Phys. Chem.*, vol. 24, no. 4, pp. 318–322.
- Glushko, V. P., L. V. Gurvich, G. A. Bergman, I. V. Veitz, V. A. Medvedev, G. A. Khachkuruzov, V. S. Youngman (1978–1982). Thermodynamic properties of individual substances, M.: Nauka.
- Kozhina, E. L. (1990). A thermodynamic properties of melts of potassium silicate system, *Russ. Phys. Chem. Glasses*, v. 16, no. 5, pp. 678–684.
- Kracek, F. C., N. L. Bowen, G. W. Morey (1937). Equilibrium relations and factors influencing their determination in the system $K_2SiO_3-SiO_2$, *J. Phys. Chem.*, vol. 41, no. 9, pp. 1183–1193.
- Shakhmatkin, B. A., N. M. Vedishcheva (1994). Thermodynamic studies of oxide glass-forming liquids by the electromotive force method, *J. Non-Cryst. Solids*, vol. 171, no. 1, pp. 1–30.
- Shornikov, S. I. (2005). Vaporization behavior and thermodynamic properties of K_2O-GeO_2 melts studied by mass spectrometry, *Russ. Inorg. Mater.*, v. 41, no. 12, pp. 1345–1356.

- Shornikov, S. I. (2009). Investigation of abilities of thermodynamic approaches on calculations of oxide activities in the compounds of the $CaO-MgO-Al_2O_3-SiO_2$ system, *Vestnik Otdelenia nauk o Zemle RAN*, vol. 27, no. 1, <http://onznnews.wdcb.ru/publications/asempg/planet-33.pdf>.
- Takahashi, K., T. Yoshio (1970). Energy relations in alkali silicates solution calorimetry, *J. Ceram. Soc. Japan*, vol. 78, no. 1, pp. 29–38.
- Zaitsev, A. I., N. E. Shelkova, N. P. Lyakishev, B. M. Mogutnov (2000). The thermodynamic properties of potassium silicates, *Russ. J. Phys. Chem.*, vol. 74, no. 6, pp. 1029–1032.